

# A Micellar Route to Layer-by-Layer Assembly of Hydrophobic Functional Polymers

Qi Bo, Xia Tong, Yi Zhao, and Yue Zhao\*

Département de chimie, Université de Sherbrooke, Sherbrooke, Québec, Canada J1K 2R1

Received February 13, 2008; In Final Form March 21, 2008;

Revised Manuscript Received March 12, 2008

**ABSTRACT:** We demonstrate a general approach to introduce hydrophobic functional polymers into a multilayer film using the layer-by-layer (LBL) assembly method that normally works for water-soluble polyelectrolytes. To this end, two new amphiphilic diblock copolymers each containing a hydrophobic side-chain liquid crystalline polymer (SCLCP) were synthesized using atom transfer radical polymerization, followed by a modification reaction. They are poly(acrylic acid)-*b*-poly{6-[4-(4'-cyanophenyl)phenoxy]hexyl methacrylate} (PAA-*b*-PCMA) and quaternized poly(4-vinyl pyridine)-*b*-poly{6-[4-(4-ethyloxyphenylazo)phenoxy]hexyl methacrylate} (QP4VP-*b*-PAMA). We show that through the use of their micelles in aqueous solutions, which have a polycation (QP4VP-*b*-PAMA) or a polyanion (PAA-*b*-PCMA) corona, the two hydrophobic SCLCPs can be LBL assembled. The characterization results indicate that the LC phases are retained in the film, and that the SCLCPs are subjected to confinement effects inside the nanodomains defined by the core regions of the micelles. This micellar route to LBL assembly of hydrophobic functional polymers is general and offers new possibilities of designing nanostructured materials.

## Introduction

Our group<sup>1</sup> and others<sup>2,3</sup> recently reported the use of the layer-by-layer (LBL) technique to assemble directly two different polymer micelles having respectively a polycation and a polyanion corona. With respect to studies of LBL assembling a polymer micelle with a molecularly dissolved polyelectrolyte,<sup>4</sup> this new development may widen our horizon in exploiting polymer micelles for the fabrication of nanostructured thin films. Of particular interest is the micellar route to introducing hydrophobic functional polymers in LBL multilayer films. In simplistic terms, in aqueous solution, the micelle of an amphiphilic diblock copolymer composed of a polyelectrolyte and a hydrophobic polymer is like a nanoparticle of the latter coated with the former. The polyelectrolyte “coating” enables the hydrophobic polymer to be assembled in a LBL fashion on a substrate, which otherwise is undoable. It is expected that this general approach of LBL assembling hydrophobic polymers could offer new possibilities for the design and development of nanostructured functional materials.

In our previous study,<sup>1</sup> we investigated the possibility of organizing two hydrophobic dyes (Nile Red and pyrene) through their pre-encapsulation in two diblock copolymer micelles, namely, the micelle with a core of poly(4-vinyl pyridine) (P4VP) and an anionic corona of poly(acrylic acid) (PAA, at pH > 7) and the micelle with a core of poly(*tert*-butyl acrylate) (PtBA) and a cationic corona of quaternized P4VP (QP4VP). The study showed that despite the apparent increase in the amounts of the two dyes with increasing number of layers, they could not be spatially separated because they are redistributed during the film buildup process through release and reabsorption in the dipping micellar solutions. An obvious solution to this problem of lack of spatial control is to covalently link the dyes to the hydrophobic polymers.

In the present work, we synthesized two new amphiphilic diblock copolymers and studied the LBL assembly of their micelles in aqueous solution. As shown in Figure 1, the two copolymers are poly(acrylic acid)-*b*-poly{6-[4-(4'-cyanophenyl)-

phenoxy]hexyl methacrylate} (PAA-*b*-PCMA) and quaternized poly(4-vinyl pyridine)-*b*-poly{6-[4-(4-ethyloxyphenylazo)phenoxy]hexyl methacrylate} (QP4VP-*b*-PAMA). While keeping the same pairing of polycation (QP4VP) and polyanion corona (PAA at pH > 7) as in the previous study<sup>1</sup> for electrostatic interactions between the two micelles, here the two hydrophobic blocks were chosen to be side-chain liquid crystalline polymers (SCLCPs) and one of them has the photoisomerisable azobenzene dye as its mesogenic side-group. In addition to extend the LBL assembly to polymer micelles with covalently bound dyes, the primary purpose of this study is to demonstrate the introduction of functional hydrophobic polymers, such as SCLCPs, into multilayer films using the LBL method. This micellar approach is different from the use of molecularly dissolved cationic and anionic SCLC ionomers (random copolymers) in constructing LC multilayers as reported by Zentel et al.<sup>5</sup> We also mention that block copolymers containing a SCLCP have been the subject of many studies on, among other things, the interplay between the liquid crystalline order and microphase separation-induced morphology.<sup>6</sup>

## Experimental Section

**1. Synthesis.** *1.1. Materials.* Unless otherwise stated, all reagents used in the syntheses were purchased from Aldrich. 4-Vinylpyridine (4VP) was dried over CaH<sub>2</sub> and distilled before use. *tert*-Butyl acrylate (*t*BA) was purified by vacuum distillation. CuCl (99.98%) was stirred in glacial acetic acid, washed with methanol and dried in vacuum; 1,1,4,7,10,10-hexamethyltriethylenetetramine (HMTETA), *N,N,N',N',N''*-pentamethyldiethylenetriamine (PMDETA), trifluoroacetic acid, and anhydrous *N,N*-dimethylformamide were used without further purification. Dichloromethane was distilled over calcium hydride prior to use, and tetrahydrofuran (THF) was used after distillation over sodium. More synthetic details for the preparation of the two amphiphilic diblock copolymers using atom transfer radical polymerization (ATRP) are given below.

*1.2. Synthesis of QP4VP-*b*-PAMA.* The synthetic route to this amphiphilic diblock copolymer is depicted in Scheme 1. Chlorine-terminated P4VP macroinitiator, P4VP-Cl, was first prepared and then used to polymerize the azobenzene monomer, 6-[4-(4-ethyloxyphenylazo)phenoxy]hexyl methacrylate (AMA),

\* Corresponding author. E-mail: yue.zhao@usherbrooke.ca.

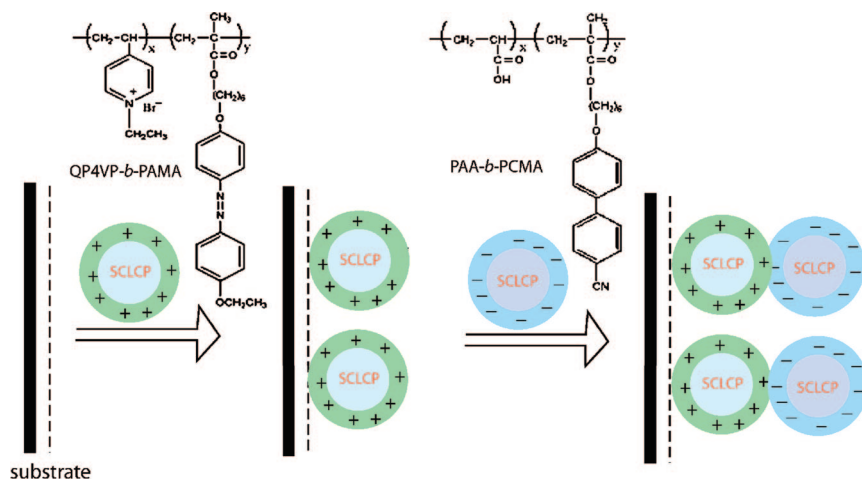
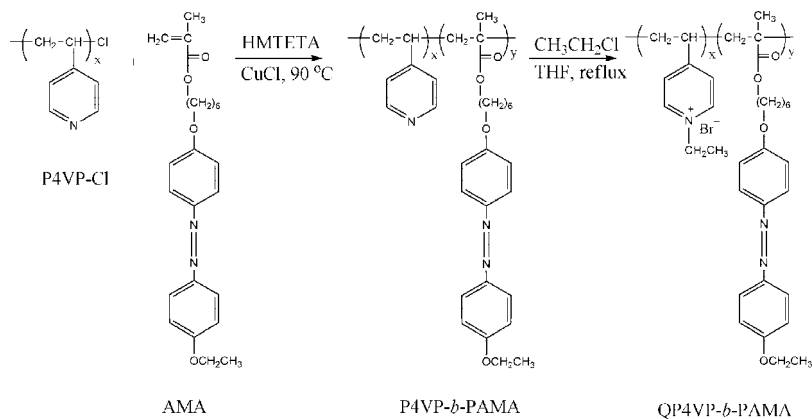


**Figure 1.** Chemical structures of the two side-chain liquid crystalline amphiphilic diblock copolymers and the schematic illustration of the layer-by-layer assembly of their micelles in aqueous solution.

### Scheme 1. Synthetic Route to QP4VP-*b*-PAMA



to yield P4VP-*b*-PAMA. The P4VP block was subsequently quaternized by reaction with bromoethane<sup>7</sup> to give QP4VP-*b*-PAMA. The syntheses of P4VP-Cl<sup>8</sup> and the azobenzene methacrylate monomer<sup>9</sup> were carried out following literature methods and are not repeated here.

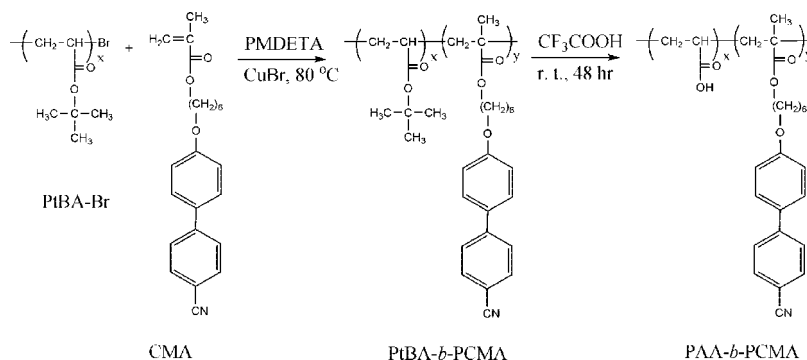
To obtain P4VP-*b*-PAMA, the macroinitiator P4VP-Cl (0.45 g,  $4.3 \times 10^{-3}$  mol of 4VP monomer units), CuCl (10 mg,  $1 \times 10^{-4}$  mol), CuBr<sub>2</sub> (2 mg,  $8.5 \times 10^{-6}$  mol), and the azobenzene monomer (0.54 g,  $1.3 \times 10^{-3}$  mol) were added to a dried round-bottom flask with a magnetic stirring bar. Then, DMF (6 mL) and HMTETA (23 mg,  $1 \times 10^{-4}$  mol) were added in succession. The reaction mixture was degassed through three freeze-pump-thaw cycles. The flask was sealed under vacuum and then immersed in an oil bath thermostatted at 90 °C; the reaction proceeded for 24 h. Afterward, the reaction mixture was diluted in THF and passed through an alumina column. The block copolymer was further purified by precipitation in ether and dried under vacuum at 40 °C (yield ~ 60%). Unlike the macroinitiator P4VP-Cl, the diblock copolymer was soluble in THF, and the GPC measurement yielded the values  $M_n = 7500$  g mol<sup>-1</sup> and  $M_w/M_n = 1.24$ . On the basis of this  $M_n$  value, the <sup>1</sup>H NMR spectral analysis gave a block copolymer composition of P4VP<sub>22</sub>-*b*-PAMA<sub>13</sub>. However, since the GPC-based molecular weight of P4VP-containing polymers is likely to be estimated lower due to the strong interaction between the pyridine groups and GPC columns with THF as eluent,<sup>10</sup> the actual size of the block copolymer may be larger.

For the quaternization of the P4VP block, P4VP-*b*-PAMA (0.5 g) and bromoethane (2 g, which is a 10-fold excess with

respect 4VP groups in the copolymer) were dissolved in 50 mL of dry THF under reflux for 48 h. The initially transparent solution turned opaque at the end of reaction. The quaternized diblock copolymer, QP4VP-*b*-PAMA, was recovered after complete removal of all solvents including bromoethane by heating (50 °C) overnight under reduced pressure. The infrared spectrum of a thin film of the collected polymer showed quaternization of P4VP, displaying a new absorption band at 1460 cm<sup>-1</sup> due to pyridinium and the concomitant disappearance of the 1414 cm<sup>-1</sup> band from pyridine.<sup>7</sup> On the basis of the decrease of the 1414 cm<sup>-1</sup> band with respect to bands unaffected by the quaternization reaction, an estimated quaternization degree of 95% was obtained.

**1.3. Synthesis of PAA-*b*-PCMA.** As shown in Scheme 2, the synthesis of this diblock copolymer also consisted in two steps. First, bromo-terminated poly(*t*-butyl acrylate) (PtBA-Br) was used to polymerize the monomer, 6-[4-(4'-cyanophenyl)phenoxy]hexyl methacrylate (CMA), to give PtBA-*b*-PCMA. Then, the PtBA block was hydrolyzed to result in PAA-*b*-PCMA.<sup>11</sup> Likewise, since the syntheses of the macroinitiator PtBA-Br<sup>8</sup> and the monomer CMA for the liquid crystalline PCMA<sup>12</sup> were carried out using literature methods, what follow are only more details on the preparation of the amphiphilic block copolymer.

To prepare PtBA-*b*-PCMA, PtBA-Br (0.68 g,  $1.7 \times 10^{-4}$  mol,  $M_n = 4000$  from GPC), CMA monomer (0.8 g,  $2.2 \times 10^{-3}$  mol), CuBr (24 mg,  $1.7 \times 10^{-4}$  mol), and CuBr<sub>2</sub> (2 mg,  $8.5 \times 10^{-6}$  mol) were charged to a dried round-bottom flask. PMDETA (30 mg,  $1.7 \times 10^{-3}$  mol) and DMF (5 mL) were then added with stirring. After being degassed by three

Scheme 2. Synthetic Route to PAA-*b*-PCMA

freeze–pump–thaw cycles, the reaction mixture was sealed in the flask under vacuum and placed in an oil bath at 80 °C. After 24 h of reaction, the mixture was diluted with THF and passed through an alumina column. The block copolymer was further purified through three precipitations in a water/methanol mixture (1/3, v/v) and dried under vacuum. GPC measurements using polystyrene standards yielded  $M_n = 24\,000$  and  $M_w/M_n = 1.28$ . The composition PtBA<sub>31</sub>-*b*-PCMA<sub>60</sub> was estimated according to the <sup>1</sup>H NMR spectrum of the copolymer using the number-average molecular weight of GPC.

The amphiphilic diblock copolymer PAA-*b*-PCMA was then obtained by hydrolysis of PtBA-*b*-PCMA. In a typical reaction, PtBA-*b*-PCMA (0.9 g) was dissolved in CH<sub>2</sub>Cl<sub>2</sub> (20 mL), followed by the addition of a 5-fold molar excess (with respect to the amount of *t*-butyl groups in the copolymer) of CF<sub>3</sub>COOH (2 g). The reaction mixture was stirred at room temperature for 24 h. Finally, after removal of most of the solvent by evaporation under reduced pressure, the block polymer PAA-*b*-PCMA was collected through precipitation in ether and dried in a vacuum oven at 40 °C. Complete hydrolysis of *t*-butyl groups was confirmed by <sup>1</sup>H NMR spectroscopy.

Here, we make a note on the purity of the samples. The two starting diblock copolymers synthesized using ATRP were purified using the standard techniques as mentioned above (passing through an alumina column, followed by precipitation). They were then subjected to the modification reaction (quaternization or hydrolysis) with the resulting amphiphilic diblocks purified again, and as described below, QP4VP-*b*-PAMA and PAA-*b*-PCMA were used to make dilute micellar solutions. Under these conditions, it is reasonable to assume that any trace amounts of transition metal/ligand that remained in the block copolymers after ATRP synthesis would not affect significantly the characterization of physical properties, the formation of micelles, or their LBL study.

## 2. Preparation of Micellar Solutions and LBL Assembly.

Micelles of both block copolymers dispersed in aqueous solution were utilized for the LBL buildup. The same procedure was

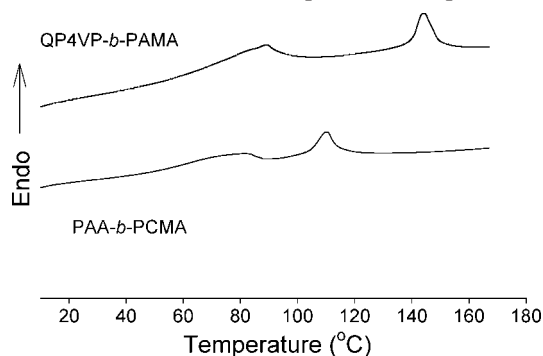


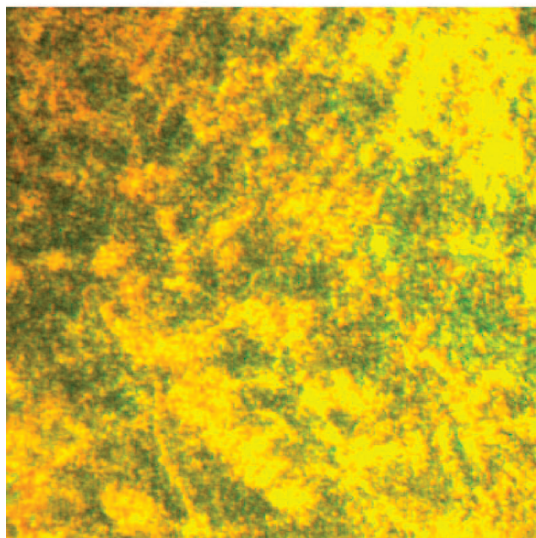
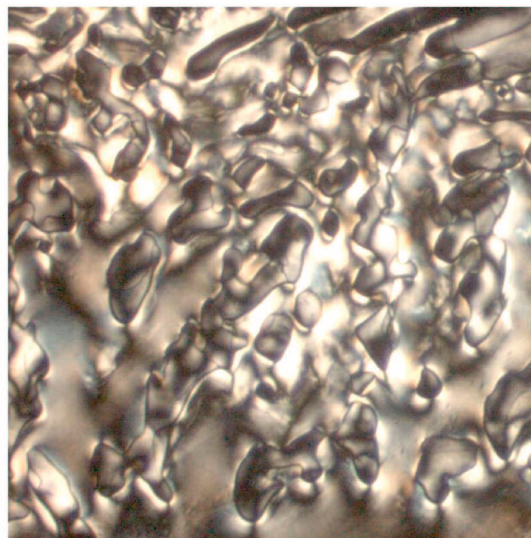
**Figure 2.** DSC heating curves (second scan) of the two amphiphilic diblock copolymers.

used to prepare the two micellar solutions. Either of the block copolymers (0.8 mg mL<sup>-1</sup> for QP4VP-*b*-PAMA or 1.0 mg mL<sup>-1</sup> for PAA-*b*-PCMA) was first dissolved in *N,N*-dimethyl formamide (DMF), and then deionized water at pH = 12 (adjusted using 1 M NaOH) was added to the DMF solution to induce the micellization; 30% of water (v/v with respect to DMF) was added at a rate of 1 drop every 20 s. The resulting micellar solution was dialyzed against deionized water with pH = 12 to remove DMF (dialysis tubing from Spectra/Por, cutoff molecular weight 3500). Finally, the micellar solution was filtered through a 0.45 μm membrane.

The LBL assembly of two polymer micelles was performed manually by repeating the typical cycle of dipping, rinsing, and drying. The two initial (as-prepared) micellar solutions were diluted to one-half of their concentrations using deionized water (pH = 12) prior to use for LBL buildup. A cleaned substrate was first dipped in the micellar solution of QP4VP-*b*-PAMA for 15 min. After rinsing with water and drying by airflow, it was dipped in the micellar solution of PAA-*b*-PCMA for 15 min, followed by rinsing and drying. The cycle was repeated to obtain the desired number of QP4VP-*b*-PAMA/PAA-*b*-PCMA bilayers. Two types of substrates (quartz and mica) were employed in this study. Quartz was treated with hydrogen peroxide and sulfuric acid (3/7, v/v) for 1 h (negatively charged surface), while muscovite mica was hand cleaved before the experiment without further treatment. For some experiments discussed in the paper, thin films of the two block copolymers containing no micelles were obtained by solution casting, followed by drying in a vacuum oven. DMF was used to dissolve QP4VP-*b*-PAMA and THF used for PAA-*b*-PCMA.

**3. Characterizations.** The diblock copolymers containing a SCLCP were characterized using a number of techniques. <sup>1</sup>H NMR spectra were recorded on a Bruker spectrometer (250 MHz, AC 250). Molecular weights and polydispersity were measured using a Waters gel permeation chromatograph (GPC) equipped with a refractive index detector (with polystyrene standards, THF eluent, and elution rate of 0.5 mL min<sup>-1</sup>). Thermal behaviors were investigated using a Perkin-Elmer DSC-7 differential scanning calorimeter (with a heating and cooling rate of 10 °C min<sup>-1</sup>). Polarizing optical microscopic (POM) observations were made on a Leitz DMR-P microscope equipped with an Instec hot stage. UV–vis spectra were recorded with a HP 8452A diode array spectrophotometer. The surface of LBL assembled multilayer films of micelles was examined using a Hitachi S-4700 field-emission-gun scanning electron microscope (SEM) operating at 3 KV as well as a Nanoscope 3A atomic force microscope (AFM) in tapping mode.

Quartz crystal microbalance (QCM) measurements were carried out using an apparatus from Resonant Probes GmbH (Germany) equipped with a sample holder (Maxtek, CHT 100, CA). Data from the network analyzer (Agilent, Palo Alto, CA,

QP4VP-*b*-PAMAPAA-*b*-PCMA

**Figure 3.** Polarizing optical micrographs for solution-cast films of QP4VP-*b*-PAMA (100 °C) and PAA-*b*-PCMA (103 °C). The image area is 244  $\mu\text{m}$   $\times$  244  $\mu\text{m}$ .

HP4396A) was analyzed using the software from Resonant Probes. The gold-coated QCM resonator was treated with  $\text{H}_2\text{SO}_4/\text{H}_2\text{O}_2$  (3:1, v/v) for 15 min, rinsed with pure water, and dried with nitrogen gas. It was then immersed in an ethanol solution of 3-mercaptopropionic acid (10 mM) for 5 h, followed by rinsing with ethanol and drying with nitrogen gas. The LBL process with the QP4VP-*b*-PAMA and PAA-*b*-PCMA micellar solutions as described above was applied with the QCM resonator. The frequency change was monitored after deposition of each bilayer of polymer micelles. All measurements were made at 3 harmonics (15, 25, and 35 MHz corresponding to the overtone  $n = 3, 5,$  and  $7,$  respectively; the fundamental frequency of the crystal is 5 MHz). Since the same results were obtained, only data with 15 MHz are shown.

For the kinetic measurements of the reversible trans-cis photoisomerization of azobenzene mesogens in the multilayer film of micelles, low intensity UV ( $\sim 365$  nm and  $1 \text{ mW cm}^{-2}$ ) and visible light irradiation ( $\sim 440$  nm and  $2 \text{ mW cm}^{-2}$ ) were obtained using a UV-vis spot curing system (Novacure) combined with filters and by adjusting the distance between the light source and the sample. By contrast, for the experiment of photoinduced alignment of azobenzene mesogens in the film, higher-intensity unpolarized UV light ( $\sim 365$  nm and  $20 \text{ mW cm}^{-1}$ ) and linearly polarized visible light ( $\sim 440$  nm and  $10 \text{ mW cm}^{-2}$ ), produced by the same curing system, were utilized.

### Results and Discussion

The two diblock copolymers synthesized using ATRP (P4VP-*b*-PAMA and PtBA-*b*-PCMA) and their amphiphilic counterparts after the respective quaternization and hydrolysis modification (QP4VP-*b*-PAMA and PAA-*b*-PCMA) were characterized (Supporting Information). First, we wanted to make sure that the liquid crystalline phases of the two SCLCPs were retained in these two amphiphilic diblock copolymers of QP4VP-*b*-PAMA and PAA-*b*-PCMA used for the LBL assembly through the use of their micelles in aqueous solution. Figure 2 shows the DSC heating curves (second scan) of the two block copolymers. For QP4VP-*b*-PAMA, like the homopolymer PAMA,<sup>13</sup> two endothermic mesophase transition peaks can be seen at about 85 and 145 °C, which should correspond to the smectic-to-nematic and nematic-to-isotropic phase transition, respectively. In the case of PAA-*b*-PCMA, the endothermic peak

appearing at about 116 °C should be the smectic-to-isotropic phase transition based on the LC phase behavior known for PCMA.<sup>14</sup> With the solution-cast films containing no micelles, on cooling slowly from the isotropic phase, birefringent textures could be observed on a polarizing optical microscope, as shown in Figure 3 for QP4VP-*b*-PAMA (100 °C) and PAA-*b*-PCMA (103 °C). These characterization results confirm that these are two SCLC amphiphilic block copolymers.

Having no surface potential analyzer to measure the actual charges of the micelles, the LBL assembly process was proceeded using aqueous micellar solutions at pH = 12. Under this condition, the carboxylic acid groups of PAA are fully ionized giving the PAA-*b*-PCMA micelle a negatively charged corona. As for the QP4VP-*b*-PAMA micelle, it has a positively charged corona since the quenched polyelectrolyte QP4VP is not affected by the basic pH. The results in Figure 4 indicate that the films of the two micelles grows in the LBL fashion. Figure 4a presents the recorded UV-vis spectra with increasing number of layers. To assess the characteristic absorption band of each copolymer, the inset shows the separate UV-vis spectra of the films of the two block copolymers cast from their corresponding micellar solutions. While QP4VP-*b*-PAMA displays the absorption maximum of azobenzene groups in the trans form around 360 nm, PAA-*b*-PCMA shows the absorption of biphenyl groups near 310 nm. The overlap of these two absorption bands (in the 300–400 nm region) for the LBL-assembled multilayer film can be noticed. Given in Figure 4b are two plots of absorbance vs number of layers. In one, the absorbance at 365 nm (azobenzene) is plotted as a function of the odd number of layers, i.e., after each deposition of QP4VP-*b*-PAMA on top, while in the other curve, the absorbance at 300 nm (biphenyl) is plotted vs the even number of layers after each deposition of PAA-*b*-PCMA on top. The two wavelengths (365 and 300 nm) are chosen to minimize the effect of overlap. From the two plots, it is clear that the amount of both polymer micelles increases almost linearly with increasing number of layers. This result shows the effectiveness of using the LBL method to assemble the two polymer micelles, each of which contains a SCLCP in the micellar core region, into a multilayer film.

In the QCM measurements, the amount of polymers of each deposited bilayer,  $\Delta m$ , is related to the frequency shift through

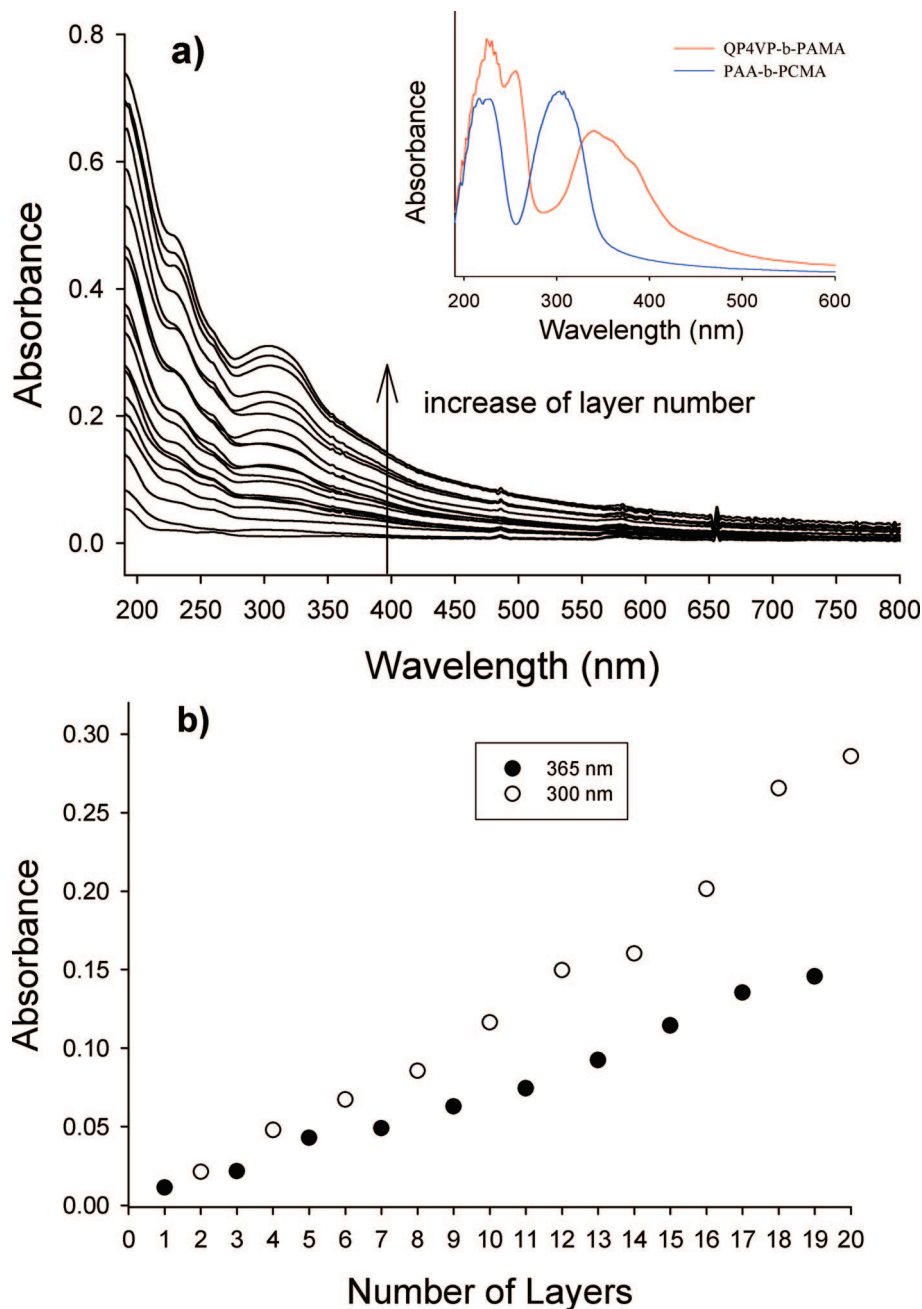


**Figure 4.** (a) UV-vis spectra of LBL assembled QP4VP-*b*-PAMA (odd numbers) and PAA-*b*-PCMA (even numbers) up to 10 bilayers. The inset shows the UV-vis spectra of separate QP4VP-*b*-PAMA and PAA-*b*-PCMA films cast from their micellar solutions. (b) Plots of absorbance at 360 nm vs odd number and of absorbance at 300 nm vs even number of layers, showing the nearly linear increase in the amount of the two polymer micelles.

$\Delta m = -C\Delta F/n$ , where  $n$  is the overtone and  $C$  is the mass sensitive constant ( $C = 17.7 \text{ ng cm}^{-2} \text{ Hz}^{-1}$ ). Figure 5 shows the plot of the frequency shift (normalized by the overtone) vs the number of polymer micelle bilayers. The general trend agrees with Figure 4. It is seen that the mass adsorbed on the substrate is smaller for the first three bilayers. With the assumption of a density of  $1.2 \text{ g cm}^{-3}$  for the polymers,<sup>15</sup> the thickness of each deposited bilayer could be calculated from the frequency shift, as shown in the inset. The result gives a thickness of about 340 nm for the 10-bilayer film of polymer micelles. The thickness as estimated from the QCM measurement is further confirmed by direct TEM observations. Figure 6 shows the cross-sectional TEM image obtained from a microtomed section of a 10-bilayer film embedded in epoxy resin. Without staining, the film can clearly be seen, and on closer inspection, even particle-like domains can also be noticed.

While the rough boundaries between the film and the epoxy as well as the seemingly irregular cross section of the film are caused by the microtoming, the average thickness is in the range of 350–400 nm, in reasonable accordance with the value calculated from QCM.

SEM observations found polymer micelles on the surface of the multilayer film. Figure 7a is the image of a film with 10 bilayers of QP4VP-*b*-PAMA/PAA-*b*-PCMA, with PAA-*b*-PCMA on top; Figure 7b is the image of the same film after deposition of an extra layer of QP4VP-*b*-PAMA on top. In both cases, micelles, most of which have diameters in the 35–40 nm range, are clearly visible. However, the coalescence and fusion of micelles can also be noticed in some areas of the films, particularly with PAA-*b*-PCMA on top (Figure 7a). As shown in Figure 8a, larger-area AFM imaging ( $10 \mu\text{m} \times 10 \mu\text{m}$ ) revealed a rough surface of the film with 10 bilayers of the

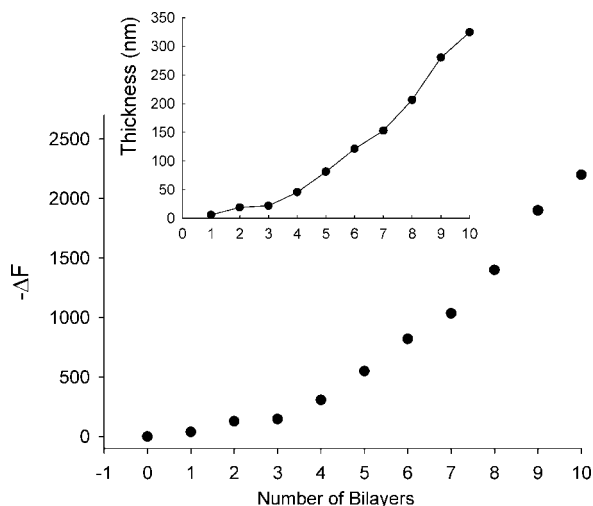


**Figure 5.** QCM frequency shift as a function of the number of deposited bilayers of QP4VP-*b*-PAMA/PAA-*b*-PCMA micelles; the inset shows the increase in thickness.

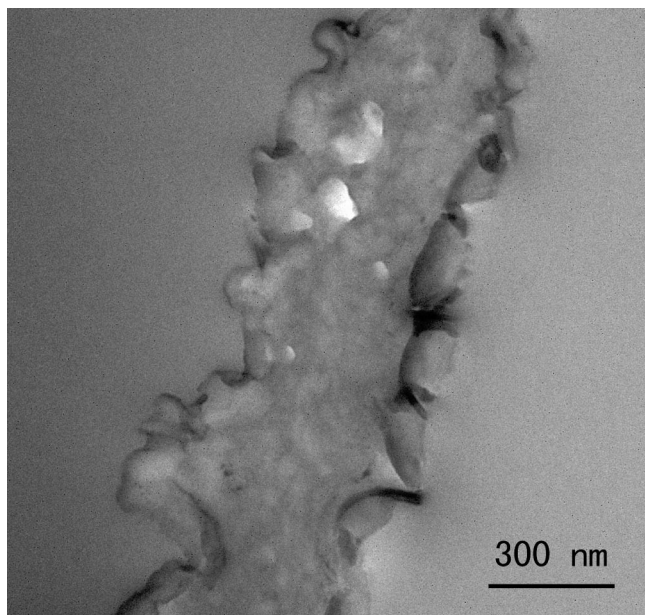


**Figure 6.** TEM cross-sectional image of a 10-bilayer film of QP4VP-*b*-PAMA/PAA-*b*-PCMA micelles.

micelles. The formation of large aggregates (several hundreds of nanometers) from the small micelles is recognizable. After the multilayer film was heated to 160 °C (in the isotropic phase of the two SCLCPs) for 5 min and then cooled to 90 °C for 30 min, the surface was found to be flattened; a number of individual micelles remained observable (Figure 8b).

By LBL assembling two polymer micelles with different hydrophobic cores and polyelectrolyte coronas, the important question that can be raised is how the micelles interact and organize in the multilayer film. In other words, can the micelles preserve their initial structure? The combined results of QCM, TEM, and SEM provide some answer to this question. As mentioned above, SEM shows that the two polymer micelles have an average diameter in the range of 35–40 nm. If the two micelles were stacked on top of each other like hard spheres, the film of 10-bilayers would have a thickness of 700–800 nm. However, the thickness as revealed by QCM and TEM is much smaller, about one-half of that value. This result allows us to infer that the two micelles with oppositely charged coronas interact strongly. Indeed, it is easy to picture that, driven by

the electrostatic interactions between the ionized PAA and QP4VP chains, not only the coronas of the two micelles can interdigitate but also they can form a complex layer whose thickness is much smaller than the coronas without chain complexation. At this time, we have no experimental evidence to suggest that the hydrophobic SCLCP cores could also be squished during the LBL buildup. However, if  $T_g$  of the SCLCP is close to room temperature, which is the case for PCMA,<sup>14</sup> this may happen.

The above spectroscopic and microscopic measurements confirm that the two polymer micelles with a hydrophobic core formed by a SCLCP can be assembled into a multilayer film in a controlled LBL fashion. In the multilayer film, the two SCLCPs should be located in the nanodomains defined by the core regions of their micelles. The question now is whether or not the two hydrophobic polymers confined in such nanodomains can still display LC mesophases. We performed careful polarizing optical microscopic observation on the LBL film with 10 bilayers. When the film was heated to 160 °C, it became completely dark indicating the isotropic nature of the film at this temperature. On slow cooling (1 °C/min), birefringent spots started to appear at about 130 °C revealing the formation of an ordered phase. Figure 9 shows an example of the POM image taken at 90 °C. Since the two polyelectrolytes (QP4VP and PAA) forming the corona of micelle are amorphous, the birefringent regions should come from the LC phases of PAMA and PCMA. Even though no clear LC texture is observed, which suggests very small regions of SCLCPs, the birefringent spots cannot arise from separated SCLCP micelle cores (~40 nm); there are likely larger SCLCP domains resulting from fusion of some micelles in the LBL film. Due to the nature of alternately layered nanodomains of the two SCLCPs in the LBL film, it was also difficult to distinguish their LC phases. On slow heating (1 °C/min), we found that parts of the birefringent regions melted at about 130 °C, which should correspond to the isotropization of PCMA, while the remaining birefringent spots, presumably from PAMA, disappeared totally only above 150 °C.

We found evidence that the SCLCP block in the micellar LBL film is under a greater confinement effect than in a thin, solution-cast film of the same diblock copolymer. Using the same irradiation conditions, we measured and compared the rate of photoisomerization of azobenzene moieties on QP4VP-*b*-PAMA in a LBL film with 10 bilayers of QP4VP-*b*-PAMA/PAA-*b*-PCMA and in a solution-cast film of QP4VP-*b*-PAMA. For the latter film, prior to the experiment, it was thermally annealed at 80 °C to enhance the microphase separation in the diblock copolymer, and the film thickness was controlled to display at 360 nm the similar absorbance to the LBL film in order to have a similar concentration of azobenzene moieties in the two types of films. The results are given in Figure 10. The example of UV-vis spectra in Figure 10a is meant to show the occurrence of the trans-to-cis photoisomerization of azobenzene in the LBL film. On UV light irradiation (~365 nm and 1 mW cm<sup>-2</sup>), the absorption band of azobenzene in the trans form around 360 nm ( $\pi$ - $\pi^*$  transition) decreases continuously. On visible light irradiation (~440 nm and 2 mW cm<sup>-2</sup>), the absorption band recovers its intensity as the reverse cis-to-trans isomerization takes place (spectra not shown). The UV-vis spectra of the solution-cast film of QP4VP-*b*-PAMA are not shown. From the change in absorbance at 360 nm, the rate of photoisomerization could be measured according to  $\ln A = -kt$ , with  $A = (A_\infty - A_t)/(A_\infty - A_0)$ , where  $A_0$ ,  $A_t$ , and  $A_\infty$  are the absorbance at 360 nm before irradiation, after irradiation for time  $t$ , and at the photostationary state, respectively.<sup>16</sup> Figure 10b shows the plots obtained for the two films. The plots give rise to straight lines in both cases indicating a first-order

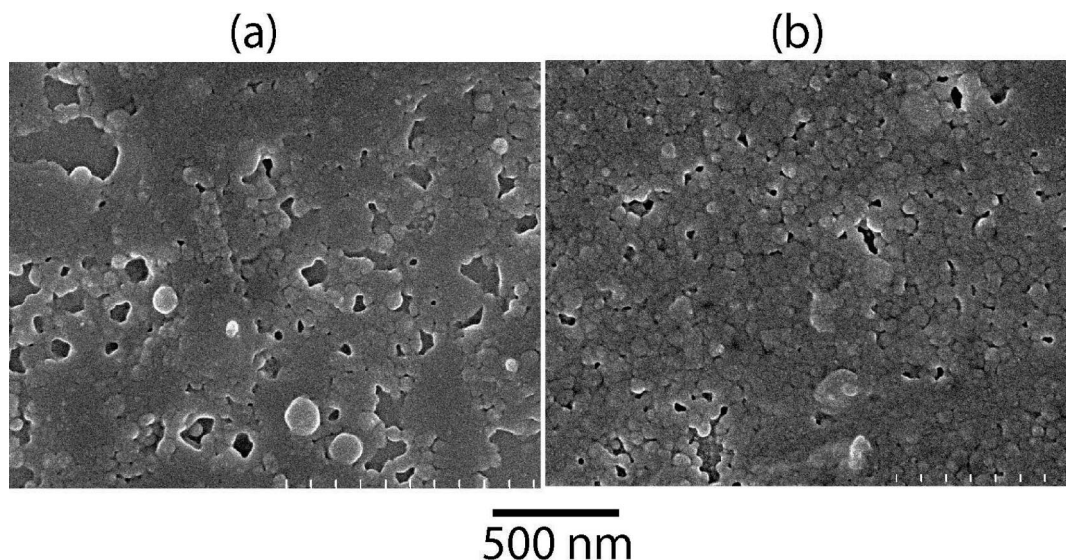


**Figure 7.** SEM images for (a) a 10-bilayer LBL film with a top layer of PAA-*b*-PCMA and (b) the film in (a) with a layer of QP4VP-*b*-PAMA deposited on top. Micelles are visible in both cases.

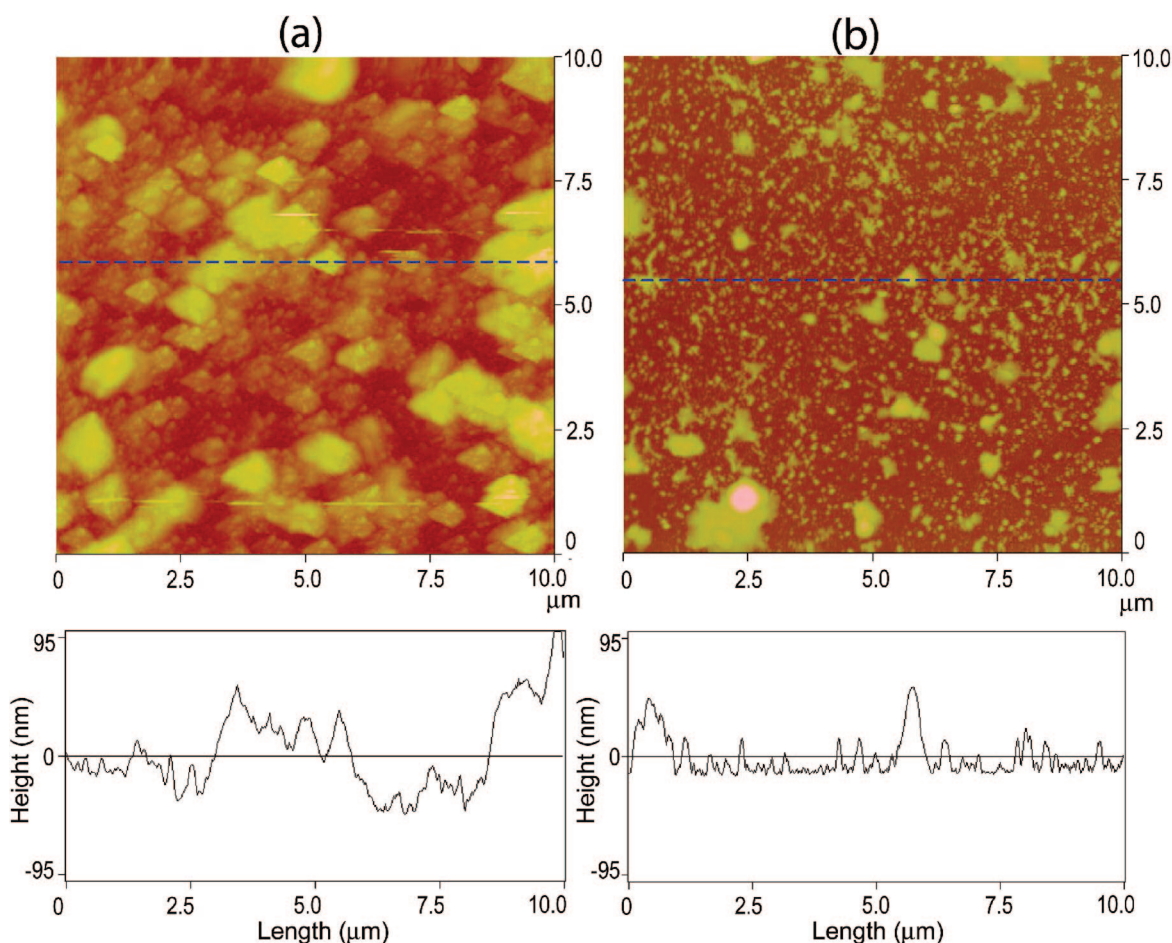


**Figure 8.** AFM images ( $10\ \mu\text{m} \times 10\ \mu\text{m}$ ) for (a) an as-prepared 10-bilayer LBL film of micelles and (b) the film in (a) after being subjected to a thermal treatment (held at  $160\ ^\circ\text{C}$  for 5 min and then cooled to  $90\ ^\circ\text{C}$  for 30 min). The height profiles correspond to the marked cross sections on the images.

photoisomerization. However, both the trans-to-cis and the cis-to-trans isomerization processes are slower in the LBL film of the two micelles than in the bulk film of QP4VP-*b*-PAMA. Despite the possible fusion of some micelles, a large part of azobenzene groups could be confined in the PAMA micelle core regions, which accounts for the slow down of photoisomerization in the LBL film. An experimental detail needs to be

mentioned here. Prior to the measurement of the rate of photoisomerization for the LBL film, the film was subjected to a cycle of UV and visible light irradiation for the reversible isomerization. We found that after this phototreatment, the absorption band of azobenzene around 360 nm became more prominent with respect to the absorption of biphenyl groups near 300 nm, which made it easier to measure the rate of

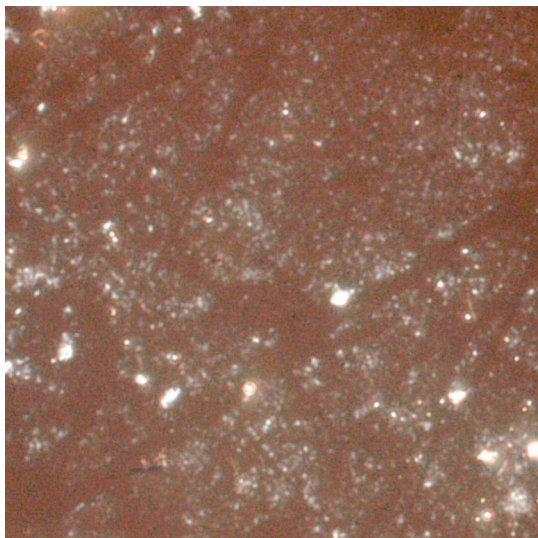


**Figure 9.** Polarizing optical micrograph for a 10-bilayer LBL film of micelles (90 °C). The image area is 146 μm × 146 μm.

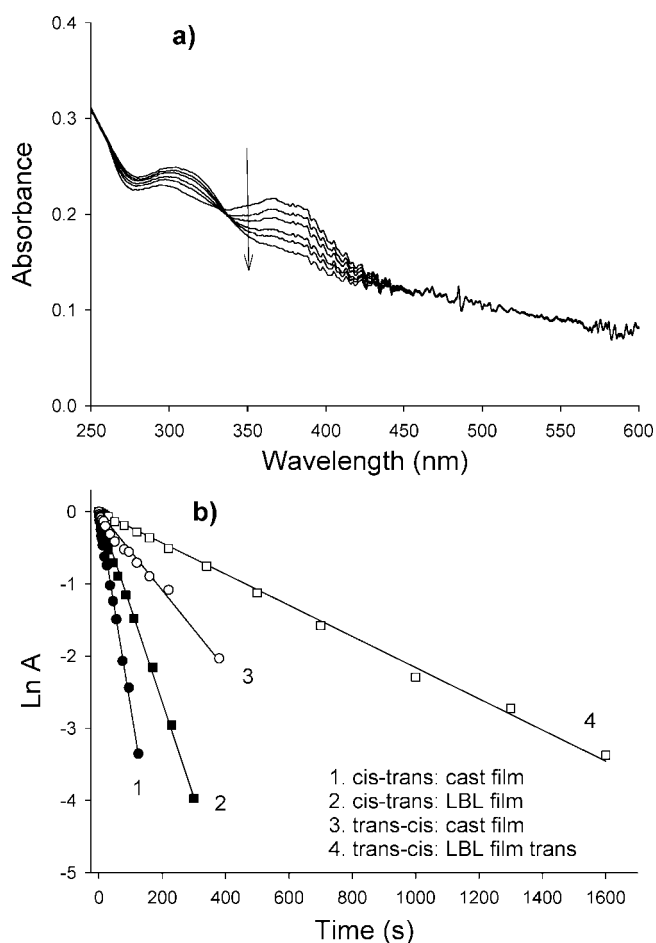


**Figure 10.** Comparison of the rates of trans-to-cis and cis-to-trans photoisomerization of azobenzene moieties occurred in a 10-bilayer LBL film of micelles and in a solution-cast film of QP4VP-*b*-PAMA (see text for details).

photoisomerization. This change can be noticed by comparing the UV-vis spectra of the as-prepared LBL film (Figure 4a) and the phototreated LBL film (Figure 10a). Such a spectral difference may reflect that a structural or morphological change has occurred in the LBL film during the pre-conducted photoisomerization process. As a note, the photoisomerization behavior

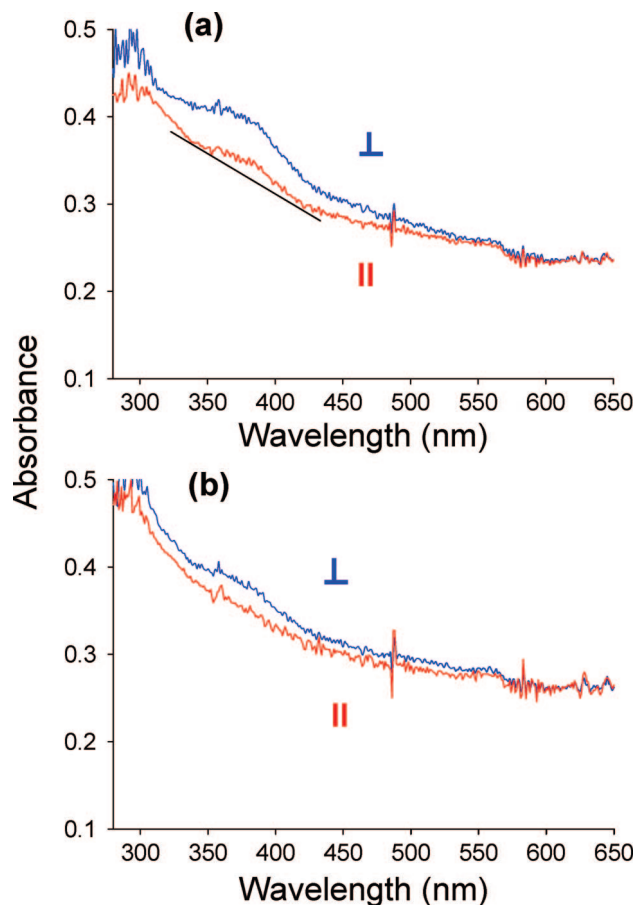


**Figure 11.** Polarized UV-vis spectra for (a) a 10-bilayer LBL film of micelles subjected to unpolarized UV irradiation followed by linearly polarized visible irradiation, showing a photoinduced orientation of azobenzene moieties (the drawing of baseline is shown) and (b) the same film after being annealed at 90 °C for 30 min. See text for details.

of QP4VP-*b*-PAMA micelles in aqueous solution was investigated and reported previously.<sup>17</sup>

Since QP4VP-*b*-PAMA contains azobenzene mesogens, we wanted to know if photoinduced orientation featured by azobenzene polymers could be obtained in the LBL film of micelles. For this experiment, the film was first exposed to unpolarized UV light to reach the photostationary state rich in cis-isomer, and then linearly polarized visible light was applied to induce the reverse cis-to-trans isomerization and the concomitant orientation of azobenzene moieties.<sup>18</sup> After this sequence of UV and visible light irradiation at room temperature, polarized UV-vis spectra were recorded with the spectrophotometer's beam polarized parallelly and perpendicular, respectively, to the polarization direction of the visible light used for the orientation induction. Figure 11a shows the spectra for the LBL film with 10 bilayers of the micelles. Even though the spectra are not of good quality due to the use of the UV polarizer, a photoinduced orientation of azobenzene moieties in the direction perpendicular to the polarization of the visible light can be noticed from the higher absorbance at around 360 nm for the perpendicular spectrum (the way to draw the baseline is shown in the figure). No dichroism was observed for the LBL film before the UV and visible light irradiation. In the case of solution-cast films of azobenzene-containing SCLC block copolymers, a subsequent thermal annealing in the LC phases could increase significantly the degree of the photoinduced orientation due to a cooperative effect of the azobenzene mesogens.<sup>19</sup> The same film in Figure 10a was held at 80 °C, above  $T_g \sim 60$  °C, for 2 h before cooling to room temperature, and Figure 11b shows the polarized spectra

recorded after the thermal treatment. Despite an apparent decrease in absorbance, the dichroism remains, if not increases slightly. This result also supports the existence of a LC phase for QP4VP-*b*-PAMA inside the micelle–core regions in the LBL film. This is because photoinduced orientation is generally relaxed in amorphous azobenzene polymers when annealed at  $T > T_g$ .<sup>20</sup> Here, it should be emphasized that we did not expect the LBL film containing SCLCPs to show specific improved LC properties. The two SCLCPs were chosen as model hydrophobic functional polymers to validate the general concept of using micelles to enable the LBL assembly of hydrophobic functional polymers.

## Conclusion

We assembled two hydrophobic SCLCPs into a multilayer film by means of the LBL method. This was made possible through the use of their micelles that contain a core of SCLCP and a corona of polyelectrolyte (polycation or polyanion) in aqueous solution. The micelles were prepared from two amphiphilic diblock copolymers, each composed of a SCLCP and a polyelectrolyte, synthesized for the purpose of LBL assembly. In the LBL film, the two SCLCPs were alternately layered and confined inside nanodomains defined by the core regions of the micelles and their LC phases were retained. The interest of this study is the demonstration of a general micellar approach that enables the use of the LBL method to assemble virtually any hydrophobic functional polymers into a thin film, with the possible nanometer-scaled control of many variables offered by the LBL technique. The extension of the robust LBL method to hydrophobic polymers would be a promising approach for new designs and development of functional nanomaterials.

**Acknowledgment.** The authors are grateful to Natural Sciences and Engineering Research Council of Canada (NSERC) and le Fonds québécois de la recherche sur la nature et les technologies of Québec (FQRNT) for financial support. They also thank Prof. Pierre Harvey, Prof. Patrick Vermette, and Mr. Charles Bertrand (University of Sherbrooke) for use of the fluorescence spectrophotometer, use of the Quartz Crystal Microbalance, and the TEM observation, respectively. Y.Z. is a member of the FQRNT-funded Center for Self-Assembled Chemical structures (CSACS).

**Supporting Information Available:** <sup>1</sup>H NMR, dynamic light scattering (DLS) and fluorescence characterizations of the block copolymers and their micelles. This material is available free of charge via the Internet at <http://pubs.acs.org>.

## References and Notes

- (1) Qi, B.; Tong, X.; Zhao, Y. *Macromolecules* **2006**, *39*, 5714.
- (2) Cho, J.; Hong, J.; Char, K.; Caruso, F. *J. Am. Chem. Soc.* **2006**, *128*, 9935.
- (3) Biggs, S.; Sakai, K.; Addison, S.; Schmid, A.; Armes, S. P.; Vamvakaki, M.; Butun, V.; Webber, G. *Adv. Mater.* **2007**, *19*, 247.
- (4) (a) Emoto, K.; Iijima, M.; Nakasaki, Y.; Kataoka, K. *J. Am. Chem. Soc.* **2000**, *122*, 2653. (b) Ma, N.; Zhang, H.; Song, B.; Wang, Z.; Zhang, X. *Chem. Mater.* **2005**, *17*, 5065. (c) Ma, N.; Wang, Y.; Wang, Z.; Zhang, X. *Langmuir* **2006**, *22*, 3906.
- (5) Choi, K.; Mruk, R.; Moussa, A.; Jonas, A. M.; Zentel, R. *Macromolecules* **2005**, *38*, 9124.
- (6) (a) See for example Poser, S.; Fischer, H.; Arnold, M. *Prog. Polym. Sci.* **1998**, *23*, 1337. (b) Mao, G.; Wang, J.; Clingman, S. R.; Ober, C. K.; Chen, J.; Thomas, E. L. *Macromolecules* **1997**, *30*, 2556. (c) Zheng, W. Y.; Albaluk, R. J.; Hammond, P. T. *Macromolecules* **1998**, *31*, 2686. (d) Schneider, A.; Zanna, J.-J.; Yamada, M.; Finkelmann, H.; Thomann, R. *Macromolecules* **2000**, *33*, 649.
- (7) Gauthier, S.; Duchesne, D.; Eisenberg, A. *Macromolecules* **1987**, *20*, 753.
- (8) Xia, J.; Zhang, X.; Matyjaszewski, K. *Macromolecules* **1999**, *32*, 3531.
- (9) Ringsdorf, H.; Schmidt, H. W. *Makromol. Chem.* **1884**, *185*, 1327.
- (10) (a) Cui, L.; Lattermann, G. *Macromol. Chem. Phys.* **2002**, *203*, 2432. (b) Qi, B.; Zhao, Y. *J. Polym. Sci., Part A: Polym. Chem.* **2006**, *44*, 1734.
- (11) Francis, R.; Lepoittevin, B.; Taton, D.; Gnanou, Y. *Macromolecules* **2002**, *35*, 9001.
- (12) Kim, K. M.; Chujo, Y. *J. Polym. Sci., Part A: Polym. Chem.* **2001**, *39*, 4043.
- (13) Yamada, M.; Itoh, T.; Nakagawa, R.; Horao, A.; Nakahama, A.; Watanabe, S. *Macromolecules* **1999**, *32*, 282.
- (14) Craig, A. A.; Imrie, C. T. *Macromolecules* **1995**, *28*, 3617.
- (15) Schuetz, P.; Caruso, F. *Adv. Funct. Mater.* **2003**, *13*, 929.
- (16) Sin, S. L.; Gan, L. H.; Hu, X.; Tam, K. C.; Gan, Y. Y. *Macromolecules* **2005**, *38*, 3943.
- (17) Qi, B.; Zhao, Y. *Langmuir* **2007**, *23*, 5746.
- (18) Cui, L.; Zhao, Y.; Yavrian, A.; Galstian, T. *Macromolecules* **2003**, *36*, 8246.
- (19) Tong, X.; Cui, L.; Zhao, Y. *Macromolecules* **2004**, *37*, 3101.
- (20) Natansohn, A.; Rochon, P. *Chem. Rev.* **2002**, *102*, 4139.

MA8003289